

RSC Advances



This is an *Accepted Manuscript*, which has been through the Royal Society of Chemistry peer review process and has been accepted for publication.

Accepted Manuscripts are published online shortly after acceptance, before technical editing, formatting and proof reading. Using this free service, authors can make their results available to the community, in citable form, before we publish the edited article. This *Accepted Manuscript* will be replaced by the edited, formatted and paginated article as soon as this is available.

You can find more information about *Accepted Manuscripts* in the [Information for Authors](#).

Please note that technical editing may introduce minor changes to the text and/or graphics, which may alter content. The journal's standard [Terms & Conditions](#) and the [Ethical guidelines](#) still apply. In no event shall the Royal Society of Chemistry be held responsible for any errors or omissions in this *Accepted Manuscript* or any consequences arising from the use of any information it contains.

Cite this: DOI: 10.1039/c0xx00000x

www.rsc.org/xxxxxx

ARTICLE TYPE

An insight into the effective advanced oxidation process for treatment of simulated textile dye waste water

Jhimli Paul Guin,^{a,*} D.B. Naik,^b Y.K. Bhardwaj^a and Lalit Varshney^a

Received (in XXX, XXX) Xth XXXXXXXXX 20XX, Accepted Xth XXXXXXXXX 20XX

DOI: 10.1039/b000000x

The efficiencies of the advanced oxidation processes (AOP) viz. photocatalysis, ozonolysis and gamma radiolysis in the absence and presence of potassium persulfate ($K_2S_2O_8$) were systematically investigated for the treatment of simulated textile dye waste water (STDWW) containing Reactive Red 120. The oxygen-equivalent chemical-oxidation capacities of photocatalysis, ozonolysis and gamma radiolysis in the absence and presence of $K_2S_2O_8$ for 16% mineralization of STDWW were calculated as 4.02, 16.19, 1.3×10^{-4} , 4.8×10^{-5} kg equiv. $O_2 m^{-3}$, respectively. The gamma radiolysis in the presence of $K_2S_2O_8$ showed the maximum extent of mineralization among these four AOPs. The pulse radiolysis studies revealed that the favourable reaction of $SO_4^{\cdot-}$ with SDBS (the most robust organic component of STDWW) producing benzyl and hydroxycyclohexadienyl type of radicals caused the enhancement in the extent of mineralization of STDWW during gamma radiolysis in the presence of $K_2S_2O_8$. The COD of the STDWW was brought down to 1558 ppm from 3128 ppm by gamma radiolysis at 50 kGy dose in the presence of $K_2S_2O_8$; though that index could not meet the allowed discharge limit ($COD \leq 250$ ppm) of industrial effluent in the main water stream. Conversely, on replacing organic acid (CH_3COOH) by inorganic acid (H_2SO_4) in the pH adjustment step, COD of STDWW was brought down to 245 ppm by gamma radiolysis at 60 kGy in the presence of $K_2S_2O_8$. This paper recommends the using of H_2SO_4 in place of CH_3COOH in the pH adjustment step followed by the gamma radiolysis of STDWW in the presence of $K_2S_2O_8$ for an effective effluent treatment.

1. Introduction

The textile industries are vital to the Indian economy as textile represents more than 10% of the country's exports. The textile effluents are a threat to the ecosystem from two perspectives; firstly, the bio-resistant synthetic dye molecules implement intense colour to water even at very low concentrations. Secondly, the auxiliary chemicals (i.e., surfactants, sequestering agent, pH-adjusting acids, inorganic salts etc.) of the dye bath contribute to ~83% of the organic load of the effluent.^{1,2} The heavy organic load of the textile effluent causes a negative impact to the aquatic lives owing to the decrease in the dissolved oxygen (DO) concentration in the water stream.³ The chemical oxygen demand (COD), which is a measure of the organic load of the effluent, varies in the ranges 2900 – 3000 ppm in the textile effluents. Since it is well above the permissible discharge limit ($COD \leq 250$ ppm) set by the Central Pollution Control Board under the Ministry of Environment and Forest, Government of India, the development of an effective and efficient treatment process for textile effluents is necessitated.

The synthetic reactive azo dyes are mostly being used in the textile industries,⁴ but those are non-reusable because of their hydrolysis in the alkaline dye bath solution. The physicochemical treatments, such as precipitation, coagulation, reverse osmosis,

electrolysis and adsorption are being used in the conventional dye effluent treatment plants.⁵ However, the large amount of sludge or secondary waste generation as well as the resistance of the reactive dyes to photo- or bio- or chemical- degradation are the major disadvantages of physicochemical treatment processes.⁶

The advanced oxidation processes (AOPs) are emerging out for the efficient oxidative mineralization of organic compounds in addition to minimizing the productions of sludge, secondary waste and toxic intermediates.⁷ The fenton, photocatalysis, sonolysis and ozonolysis are well studied AOPs, but suffer from their own limitations.⁷⁻¹² Radiolysis using high energy ionizing radiation is upcoming as one of the promising AOPs for the degradation of varieties of dyes and organic pollutants in aqueous solution. Decolouration and mineralization of pure Reactive Red-120 (RR-120) dye using high energy radiation (gamma and electron beam) was recently reported by us.¹³⁻¹⁴ The results showed satisfactory mineralization of RR-120 on irradiation to a dose of 10 kGy. However, the recalcitrant nature of the auxiliary organic components of textile dye bath solution demands a validation of the process efficiencies of a couple of AOPs for the mineralization of simulated textile dye waste water (STDWW), mimicking the compositions used in dye industries.

In the present study, three AOPs viz. photocatalysis, ozonolysis and gamma radiolysis were employed to evaluate the process efficiency of mineralization of STDWW. The pulse

radiolysis studies were employed to understand the mineralization of SDBS (the most robust organic component of STDWW) by $\text{SO}_4^{\bullet-}$. The oxygen-equivalent chemical-oxidation capacities (OCCs) of these AOPs were also evaluated to support the observed trends in mineralization. This is the first report, to the best of our knowledge; on the determination of OCC of photocatalysis and gamma radiolysis. The effects of different additives, neutralising acids and the change in pH of STDWW during the mineralization process were also investigated.

2. Experimental

2.1 Dye and chemicals

RR-120, sodium dodecylbenzenesulfonate (SDBS), sodium dodecyl sulfate (SDS), ethylenediaminetetraacetic acid (EDTA), $\text{K}_2\text{S}_2\text{O}_8$, *tert*-butanol were purchased from Sigma-Aldrich. The titanium dioxide (TiO_2) (Degussa (P25), particle size ~ 30 nm) was used as photocatalyst. All other chemicals used were of the highest purity and used without any pretreatment.

2.2 Preparation of STDWW

The components of the dye bath and the role of each constituent in the dyeing process are summarized in Table 1. The hydrolyzed dye effluent was prepared by boiling the constituents with 1 M NaOH at 80-90 °C for 3 h under reflux.¹⁵ The characteristic of the hydrolysed dye effluent before the treatment process is given in Table 1.

Table 1 Composition of STDWW (Chemical oxygen demand = 3128 mg/L, pH=10; Dissolved oxygen ~ 7.3 mg/L, Conductivity= 28.9 mS)

| Component | Concentration (mg/L) | Function |
|---|----------------------|--|
| C.I. Reactive Red 120 | 70 | Colouring agent |
| Sodium dodecyl benzenesulfonate (SDBS) | 375 | Detergent used for washing excess dye |
| Ethylenediamine tetraacetic acid (EDTA) | 150 | Removal of unwanted metal ions in the dye bath |
| Na_2CO_3 | 4876 | Adjustment of the starting pH (8.8-9.3) |
| NaOH | 188 | Adjustment of the final dyeing pH (10.5-11.0) |
| NaCl | 1.5×10^4 | Promotes dye binding onto cotton |
| Acetic acid | As required | For pH (10) adjustment |

2.3 Instruments and analytical procedures

Steady state radiolysis of STDWW solution was carried out at different doses using ^{60}Co gamma radiation with a dose rate of 2.0 kGy h^{-1} . The dose rate of the gamma source was determined by using Fricke dosimetry [$G(\text{Fe}^{3+}) = 15.6/100$ eV]. The photocatalytic experiments were carried out by using Rayonet Photochemical Reactor. The light source contains 16 mercury lamps of 8W power each and emitting in the near-UV (mainly around 350 nm) having initial photon flux (I_0) of 5.0×10^{15} photons $\text{cm}^{-2} \text{s}^{-1}$. The volume and area of the cell is V (cm^3) and A (cm^2), respectively. Ozone was continuously produced from pure oxygen by UOS04 model ozone generator and bubbled into

the aqueous solution of STDWW. The ozone generator can produce 4 g h^{-1} ozone from pure oxygen feed where oxygen flow rate was maintained as 2 L min^{-1} . The input rate of ozone from the ozone generator into the aqueous solution was determined as 7.3×10^{-3} mol $\text{dm}^{-3} \text{min}^{-1}$ by the standard iodometric method. Pulse radiolysis (PR) experiments were performed by optical detection measurement with 7 MeV linear electron accelerator with pulse duration of 500 ns. Dose per pulse was measured using aerated aqueous solution of thiocyanate taking (G_e) = 2.6×10^{-4} $\text{m}^2 \text{J}^{-1}$ at 475 nm.¹⁶ Decolouration, COD and pH of the solutions were measured by using U-2800 spectrophotometer, Spectroquant® Pharo 300 COD analyser and pH meter 600, respectively.

3. Results and Discussion

3.1. Decolouration and mineralization of STDWW by photocatalysis and ozonolysis

The hydroxyl radical, $\bullet\text{OH}$, which is a strong oxidising agent, is generated from the surface of TiO_2 particles upon irradiating with UV light. The photocatalytic treatment of STDWW was carried out for different time intervals. It took about 500 min of this process to completely decolorize STDWW. However, at the same time, it could mineralise only 21% of the total organic loads of STDWW (Fig. 1a). The rate of photocatalytic mineralization decreased with time. Therefore, only 25% mineralization was observed at 720 min and no significant change in the extent of mineralization was observed on prolonged irradiation.

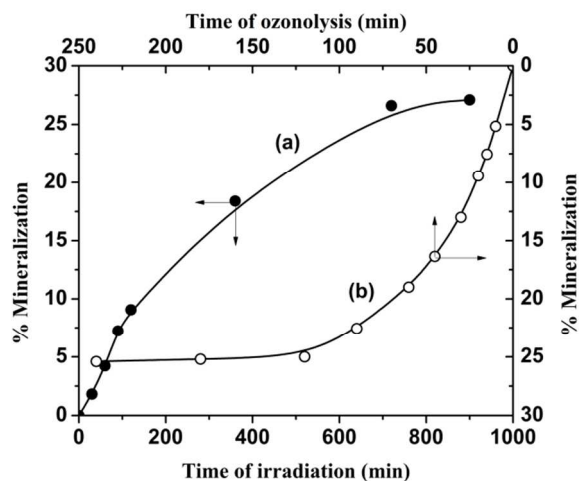


Fig. 1 Mineralization of STDWW on (a) photocatalysis (b) ozonolysis.

The TiO_2 particles made very stable suspensions with the aqueous solution of the individual components of STDWW. However, it settled down rapidly in STDWW. We speculated that the presence of high salts concentration ($\sim 2 \times 10^4$ ppm of NaCl) in the STDWW might be responsible for changing the surface properties of TiO_2 particles and it finally led to the easy settlement of the catalyst in STDWW. Since, we do not have the photoreactor with stirring facilities, we can only speculate, but could not confirm that the rapid settlement of catalyst in STDWW might be one of the reasons behind the poor efficiency of photocatalytic mineralization of STDWW. On the other hand, the coulombic repulsion between the negatively charged surface

of TiO₂ (pH_{pzc} = 6.0 ± 0.2) and OH⁻ (at pH 10.0) could also prevent the production of •OH resulting into the poor mineralization of STDWW.^{17,18}

Ozone (O₃) can be decomposed in alkaline pH (pH 10.0) producing •OH.¹⁹ O₃ is also a strong chemical oxidant and it can directly react with the unsaturations present in the organic molecules.²⁰ Therefore, O₃ and •OH both could react with the components of STDWW. However, the direct reaction of O₃ is selective and slow. The ozonolysis of STDWW was carried out for different time intervals. The complete decolouration and negligible mineralization of STDWW were observed at ~3 min of ozonolysis. About 25% mineralization of STDWW was observed after 120 min and remained almost constant at prolonged ozonolysis (Fig. 1b). The process efficiency (in terms of the % mineralization of STDWW) of ozonolysis was tried to even increase by adding some additives such as H₂O₂, Al₂O₃, K₂S₂O₈ etc., but the extent of % mineralization did not increase. The continuous flow of oxygen during ozonolysis also did not improve the extent of % mineralization of STDWW.

3.2. Decolouration and mineralization of STDWW by gamma radiolysis

Radiolysis of water in the pH range 3-11 produces three main reactive intermediates viz. hydrated electron (e_{aq}⁻), •OH radical and hydrogen atom (H). The G-values [species/100 eV] of the intermediates are given below:²¹

$$G(e_{aq}^-) = 2.7; G(\bullet\text{OH}) = 2.7; G(\text{H}\bullet) = 0.6 \quad (1)$$

Under atmospheric condition, e_{aq}⁻ and H mainly react with the dissolved oxygen producing superoxide radical anion (O₂^{•-}) and perhydroxyl radical (HO₂[•]), respectively. Therefore, •OH remains as the predominant species in aqueous solution.

The radiolysis of STDWW was carried out for different doses. The complete decolouration and negligible mineralization of STDWW were observed at ~3 kGy dose. The extent of mineralization of STDWW was increased only up to 16% at 50 kGy dose and no further enhancement in the mineralization was observed at higher doses (Fig. 2a).

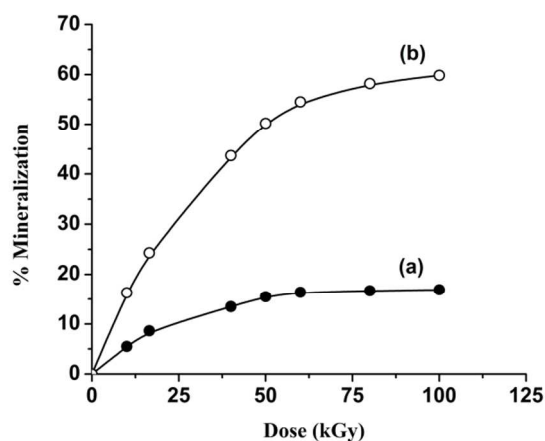
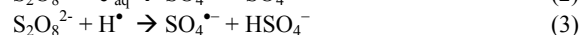
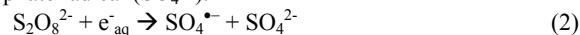


Fig. 2 Mineralization of STDWW on gamma radiolysis (a) without and (b) with K₂S₂O₈.

The above discussed results in conjugation with the results discussed in Section 3.1 suggested that •OH cannot effectively

mineralize the organic load of STDWW. Paul et al. reported an enhancement in the radiolytic mineralization of ibuprofen by gamma radiolysis in presence of K₂S₂O₈.²² The e_{aq}⁻ and H[•] preferentially reacts with S₂O₈²⁻ during radiolysis resulting into sulphate radical (SO₄^{•-}).²³



$$G(\text{SO}_4^{\bullet-}) = 3.3 \quad (4)$$

The SO₄^{•-} is itself an oxidising radical. In addition, •OH radical also can react independently with organic compounds.²⁴ The gamma radiolysis of STDWW was carried out for different doses in presence of 4 × 10⁻² mol dm⁻³ K₂S₂O₈. The % mineralization of STDWW was enhanced to 50% at 50 kGy dose, though it remained almost constant at higher doses than 50 kGy (Fig. 2b).

It is important to mention that K₂S₂O₈ itself can produce SO₄^{•-} by thermal decomposition at 38-40 °C,²⁵ which is the usual temperature of the solution during gamma radiolysis. Therefore, the extent of mineralization of STDWW in presence of 4 × 10⁻² mol dm⁻³ K₂S₂O₈ was studied at 40 °C in absence of gamma source and no mineralization of STDWW was obtained.

In this context, it is important to mention that the COD of STDWW was 3128 ppm, which was much higher than the COD of pure dye solution (50 ppm) and it indirectly represented the amount of other organic compounds (viz. SDBS, EDTA, CH₃COOH etc.) present in STDWW. After some preliminary experiments, it was found that the high value of COD was mainly contributed by SDBS, EDTA and CH₃COOH. The concentration of CH₃COOH varies from case to case as it is used to neutralize the pH of the dye bath and thus the radiolysis of pure CH₃COOH component was not investigated. The aqueous solutions of EDTA (150 ppm) and SDBS (375 ppm) were irradiated at pH 10.0 individually at a dose of 50 kGy both in the absence and presence of K₂S₂O₈. About 80% and 95% mineralization of EDTA were observed in the absence and presence of K₂S₂O₈. It suggests that EDTA can be mineralized easily by irradiation unlike SDBS. However, more interestingly, about 16% and 62% mineralization of SDBS was observed in the absence and presence of K₂S₂O₈. Therefore, the extent of mineralization of SDBS was observed to be enhanced by approximately 4 times in case of gamma radiolysis in the presence of K₂S₂O₈.

In presence of HCO₃⁻ and CO₃²⁻, the extent of mineralization of the organic components present in STDWW was expected to be decreased because of the expected scavenging of •OH radical by the HCO₃⁻ and CO₃²⁻ ions.²⁶ However, no appreciable enhancement in the extent of mineralization was observed during the radiolysis in absence of Na₂CO₃. It indicates that CO₃²⁻ might not have interfered during the radiolysis of STDWW.

3.3 Comparison of the process efficiencies of photocatalysis, ozonolysis and gamma radiolysis for the mineralization of STDWW

The process efficiencies of different AOPs were compared in the terms of OCC, which is defined as the kg of O₂ that are equivalent to the quantity of oxidant reagents used in an AOP to treat 1 m³ of wastewater.²⁷ It gives an index of the chemical efficiency of the oxidants used in an AOP by quantifying the amount of the oxidants (kgO₂) added per m³ of the wastewater. The OCC of photocatalysis, ozonolysis and gamma radiolysis are calculated by the following equations (5-7):

$$1 \text{ OCC}_{\text{Photo}} (\text{kg O}_2 \text{ m}^{-3}) = \frac{[I_0 (\text{cm}^{-2} \text{ s}^{-1}) \times A (\text{cm}^2) \times t (\text{s}) \times 1000 (\text{cm}^3 \text{ m}^{-3})]}{[6.023 \times 10^{23} (\text{kmol}^{-1}) \times V (\text{cm}^3)]} \times \frac{1 \text{ kmol O}_2}{4 \text{ kmol}} \times \frac{32 \text{ kg O}_2}{1 \text{ kmol O}_2} \quad (5)$$

$$1 \text{ OCC}_{\text{Ozo}} (\text{kg O}_2 \text{ m}^{-3}) = \text{O}_3 (\text{kg O}_3 \text{ m}^{-3}) \times \frac{1 \text{ kmol O}_3}{48 \text{ kg O}_3} \times \frac{6 \text{ kmol e}^-}{1 \text{ kmol O}_3} \times \frac{1 \text{ kmol O}_2}{4 \text{ kmol e}^-} \times \frac{32 \text{ kg O}_2}{1 \text{ kmol O}_2} \quad (6)$$

$$1 \text{ OCC}_{\text{Radio}} (\text{kg O}_2 \text{ m}^{-3}) = D (\text{J kg}^{-1}) \times \rho (\text{kg m}^{-3}) \times G (\text{kmol J}^{-1}) \times \frac{1 \text{ kmol O}_2}{4 \text{ kmol}} \times \frac{32 \text{ kg O}_2}{1 \text{ kmol O}_2} \quad (7)$$

5 Where, D is the dose, ρ is the density of water, $G(\text{SO}_4^{\bullet-}) = 3.4 \times 10^{-10} \text{ kmol J}^{-1}$ or $3.3/100 \text{ eV}$; $G(\bullet\text{OH}) = 2.8 \times 10^{-10} \text{ kmol J}^{-1}$ or $2.7/100 \text{ eV}$.

The lowest degree of mineralization (16%) of STDWW was observed for gamma radiolysis (Fig. 3). Thus the OCCs of different AOPs were compared for only 16% mineralization of STDWW and they were calculated as 4.02, 16.19, 1.3×10^{-4} , $4.8 \times 10^{-5} \text{ kg equiv. O}_2 \text{ m}^{-3}$ for photocatalysis, ozonolysis and gamma radiolysis in the absence and presence of $\text{K}_2\text{S}_2\text{O}_8$, respectively. Therefore, for the same extent of mineralization, least amount of oxidant was required for the gamma radiolysis in presence of $\text{K}_2\text{S}_2\text{O}_8$. To the best of our knowledge, this is the first report on the calculation of OCC for photocatalysis and gamma radiolysis.

Gamma radiolysis in the presence of $\text{K}_2\text{S}_2\text{O}_8$ showed better chemical efficiency (i.e. 47% mineralization) of the oxidants at OCC of $2.3 \times 10^{-4} \text{ kg equiv. O}_2 \text{ m}^{-3}$, which was equivalent to 16% mineralization for the radiation treatment in absence of $\text{K}_2\text{S}_2\text{O}_8$. Moreover, no mineralization was observed at that OCC value for both ozonolysis and photocatalysis. The overall results suggest that the gamma radiolysis in the presence of $\text{K}_2\text{S}_2\text{O}_8$ is the most efficient process for the treatment of STDWW compared to the general gamma radiolysis, photocatalysis and ozonolysis.

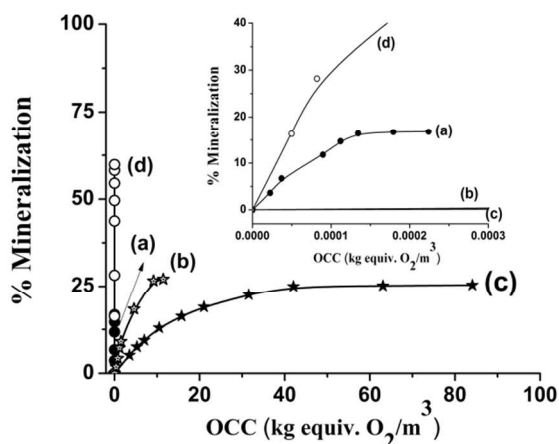


Fig. 3 Variation in mineralization extent with OCC of (a) radiolysis (b) photocatalysis (c) ozonolysis (d) radiolysis in presence of $\text{K}_2\text{S}_2\text{O}_8$. Inset: Mineralization extent at lower OCC (a) radiolysis (b) photocatalysis (c) ozonolysis (d) radiolysis in presence of $\text{K}_2\text{S}_2\text{O}_8$.

3.4 Mechanism of mineralization of the components present in STDWW

Méndez-Díaz et al. speculated that the conjugative action of $\bullet\text{OH}$ and $\text{SO}_4^{\bullet-}$ might be led to the higher extent of mineralization of SDBS during the photooxidation of SDBS in presence of $\text{K}_2\text{S}_2\text{O}_8$ at pH 7.²⁸ We want to note that the yield of oxidizing radicals in gamma radiolysis in presence of $\text{K}_2\text{S}_2\text{O}_8$ is 6

$[=G(\bullet\text{OH}) + G(\text{SO}_4^{\bullet-}) + G(\text{H}^{\bullet})]$, whereas, that in absence of $\text{K}_2\text{S}_2\text{O}_8$ is 2.7 ($=G(\bullet\text{OH})$). Therefore, ~ 2.2 times enhancement in the extent of mineralization of SDBS could be expected during gamma radiolysis in the presence of $\text{K}_2\text{S}_2\text{O}_8$ compared to the same in the absence of $\text{K}_2\text{S}_2\text{O}_8$. However, in the Section 3.2, we showed that the extent of mineralization of SDBS was enhanced by approximately 4 times due to the presence of $\text{K}_2\text{S}_2\text{O}_8$ during gamma radiolysis.

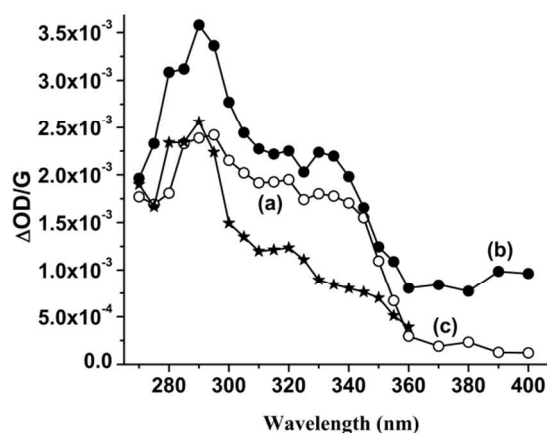
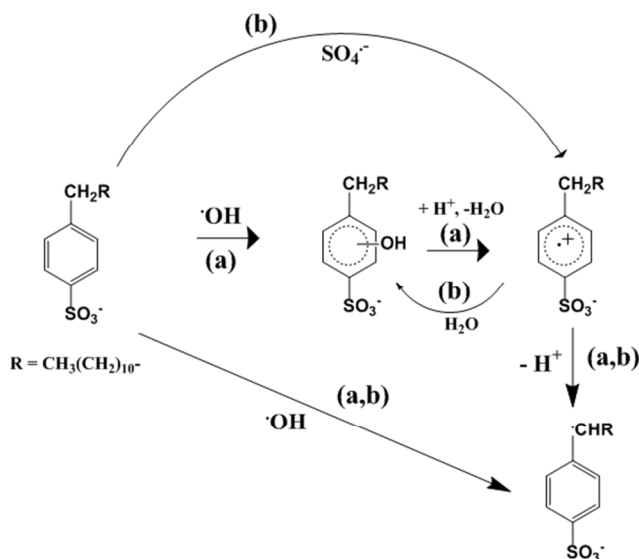


Fig. 4 Transient absorption spectra for the reaction of SDBS with (a) $\bullet\text{OH}$ (b) $\text{SO}_4^{\bullet-}$ (c) $\text{O}^{\bullet-}$ at dose of 14 Gy/pulse.

Therefore, the reactions between SDBS with $\bullet\text{OH}$ and $\text{SO}_4^{\bullet-}$ were investigated by PR experiments in $5.0 \times 10^{-4} \text{ mol dm}^{-3}$ aqueous solution of SDBS saturated with (i) N_2O and (ii) N_2 , respectively, by employing 14 Gy/pulse at pH 10.0. The $2.0 \times 10^{-2} \text{ mol dm}^{-3} \text{ K}_2\text{S}_2\text{O}_8$ and $0.02 \text{ mol dm}^{-3} \text{ tert-butanol}$ were added additionally to the solution for the second reaction. Fig. 4 shows the absorbance per unit G value ($\Delta\text{OD}/\text{G}$) of the transient species formed by $\bullet\text{OH}$ or $\text{SO}_4^{\bullet-}$ radicals as a function of wavelength. In Fig. 4a, a strong absorption at 290 nm, a weak absorption peak at 320 and a weak hump in the range of 325-340 nm was observed for the reaction between SDBS and $\bullet\text{OH}$. The peak around at 270-290 nm is attributed to the benzyl type radical and broad peak at 300-350 nm correspond to the formation of OH-adduct with the benzene ring.^{22,29} All of the transient species absorbing at 290, 320 and 325-340 nm decayed faster in presence of 4:1 (v:v) mixture of N_2O and O_2 and it suggests that the produced transient species had carbon centred radicals. The decay constant of the transient reacting with O_2 could not be determined because of the interference of the formation signal of the peroxy type radical with the decay signal of the reacting transient. Scheme 1a represents the probable routes of formation of the OH-adducts

and benzyl type radicals from the reaction between SDBS and $\cdot\text{OH}$. The $\cdot\text{OH}$ first conjugates with the benzene ring of SDBS forming the OH-adduct, which reacts with the water molecules leading to the formation of the benzene radical cation. The benzene radical cation is unstable and it forms a benzyl type radical by dissociation of the weak benzylic C_α -hydrogen.^{22,30} Both the intermediates viz. OH-adduct and benzyl type radicals are observed for the reaction of $\cdot\text{OH}$ with SDBS. Apart from these above phenomena direct H-atom abstraction may also take place from the alkyl chain of SDBS by $\cdot\text{OH}$.²⁹ The bi-molecular rate constant of the reaction between $\cdot\text{OH}$ and SDBS was calculated as $1.8 \times 10^9 \text{ dm}^3 \text{ mol}^{-1} \text{ s}^{-1}$ (at pH 10.0), which is similar to the value reported $\sim 10^{10} \text{ dm}^3 \text{ mol}^{-1} \text{ s}^{-1}$ (at pH 7) by Méndez-Díaz et al.²⁸

The similar types of transient absorption peaks were observed at 290, 320 and 330 nm in the reaction of SDBS with $\text{SO}_4^{\cdot-}$ (Fig. 4b). However, the intensity of the peak at 290 nm significantly increased by 1.5 times in case of $\text{SO}_4^{\cdot-}$ as compared to the $\cdot\text{OH}$. The $\text{SO}_4^{\cdot-}$ is more selective electrophile compared to $\cdot\text{OH}$.²⁸ Scheme 1b represents the probable routes of reaction between $\text{SO}_4^{\cdot-}$ and SDBS. The $\text{SO}_4^{\cdot-}$ does not directly add to the aromatic ring. Instead it produces a very short lived ($< 0.1 \mu\text{s}$) radical cation followed by benzyl type radical and hydroxycyclohexadienyl radical by the reactions with water molecules.^{22,31} $\text{SO}_4^{\cdot-}$ can also produce benzyl radical by H-abstraction reaction from the alkyl chain of the SDBS.^{28,32,33} The bi-molecular rate constants for the reaction of $\text{SO}_4^{\cdot-}$ with SDBS was calculated as $3.8 \times 10^8 \text{ dm}^3 \text{ mol}^{-1} \text{ s}^{-1}$ from the decay of $\text{SO}_4^{\cdot-}$ at 450 nm (at pH 10.0) and it is similar to the value reported $\sim 3.6 \times 10^8 \text{ dm}^3 \text{ mol}^{-1} \text{ s}^{-1}$.



Scheme 1 Reaction scheme of SDBS with $\cdot\text{OH}$ and $\text{SO}_4^{\cdot-}$.

The H-abstraction reaction of $\text{SO}_4^{\cdot-}$ from the alkyl chain was verified by monitoring the decay of $\text{SO}_4^{\cdot-}$ radical with the reaction of SDS in N_2 purged $5.0 \times 10^{-4} \text{ mol dm}^{-3}$ SDS containing $2.0 \times 10^{-2} \text{ mol dm}^{-3} \text{ K}_2\text{S}_2\text{O}_8$ and $2.0 \times 10^{-2} \text{ mol dm}^{-3}$ *tert*-butanol at pH 10.0 by employing 14 Gy/pulse. The decay constant of $\text{SO}_4^{\cdot-}$ for the reaction with SDS was calculated as $4.7 \times 10^5 \text{ s}^{-1}$ at 440 nm and it was found to be about 1.5 times higher compared to the decay of $\text{SO}_4^{\cdot-}$ in a solution containing no SDS (spectra is

not shown). It supports that the H-abstraction reaction of $\text{SO}_4^{\cdot-}$ from the alkyl chain of SDS and SDBS are of similar nature.

The absorption peaks of the transients formed by the reaction between SDBS and $\text{O}^{\cdot-}$ were also monitored in N_2O saturated $5.0 \times 10^{-4} \text{ mol dm}^{-3}$ aqueous SDBS solution at pH 13.5 by applying 14 Gy/pulse (Fig. 4c). The $\text{O}^{\cdot-}$, being a nucleophilic species cannot add to the benzene ring, rather it is known to react via one electron oxidation producing benzene radical cation followed by benzyl type radicals by the dissociation of C_α -hydrogen.³⁴ Therefore, it showed $\Delta\text{OD}/\text{G}$ features similar to the reaction between SDBS and $\text{SO}_4^{\cdot-}$. The higher peak intensity at 290 nm observed for the reaction between $\text{SO}_4^{\cdot-}$ and SDBS is attributed to more favourable formation of benzyl radicals by $\text{SO}_4^{\cdot-}$. Therefore, the higher extent of mineralization of SDBS is not because of the conjugative effect of both $\cdot\text{OH}$ and $\text{SO}_4^{\cdot-}$ radicals, but because of the preferential formation of benzyl type of radicals via the formation of benzene radical cation.

3.5 The influence of the nature of neutralizing acid on the radiolysis of STDWW

The pH of the STDWW solution did not appreciably change even after 50 kGy dose of radiolysis (Fig. 5a) because of the lesser extent of formation of the organic acids from the mineralization of the organic components of STDWW. On the other hand, the pH of the STDWW decreased to 6.3 on irradiating the solution in presence of $\text{K}_2\text{S}_2\text{O}_8$ for the same dose (Fig. 5b) because of the higher extent of formation of the organic acids from the mineralization of the organic components. The $\text{SO}_4^{\cdot-}$ radical efficiently oxidises the organic compounds and itself converts into SO_4^{2-} , which is a conjugate base of strong acids (HSO_4^- , H_2SO_4). Therefore, the pH of the solution significantly decreased during radiolysis in presence of $\text{K}_2\text{S}_2\text{O}_8$.³⁵ This phenomenon led to the existence of the organic acids in their protonated form and therefore, the rate constants of these acids with $\text{SO}_4^{\cdot-}$ decreased which resulted almost negligible extent of mineralization at higher doses than 50 kGy.³⁵ Moreover, the HCO_3^- ion concentration in equilibrium with CO_3^{2-} increases with decreasing the pH and it minimizes the scavenging effect as HCO_3^- .³⁶ However, the minimum COD achieved in the irradiated solution in presence of $\text{K}_2\text{S}_2\text{O}_8$ was 1776 ppm, which was much above the permissible discharge limit (≤ 250 ppm).

The acetic acid, which was used to adjust the pH of the simulated dye solution, is an organic acid and it contributes significantly in the residual COD of the irradiated solution. Therefore, we did the radiolysis of STDWW in presence of $\text{K}_2\text{S}_2\text{O}_8$ by replacing the acetic acid (organic acid) by H_2SO_4 (mineral acid) in the pH adjustment step. The STDWW solution, where the pH was adjusted by diluted H_2SO_4 will be henceforth designated as STDWW-SA. The initial CODs of the STDWW and STDWW-SA were calculated as 3128 and 1544 ppm, respectively. It could itself give an idea about the contribution of the acetic acid in the total COD of the simulated solution.

Moreover, the extent of mineralization of STDWW-SA increased to 84% upon gamma irradiation for 50 kGy in presence of $\text{K}_2\text{S}_2\text{O}_8$ and the pH of the solution drastically decreased to ~ 2.1 . Despite the incomplete mineralization, The COD of STDWW-SA could bring down to 245 ppm (which is below the recommended discharge limit) upon irradiation for ~ 60 kGy in presence of $\text{K}_2\text{S}_2\text{O}_8$. The pH of the irradiated solution was

remained constant in the range 1.5-2.0 (Fig. 5c).

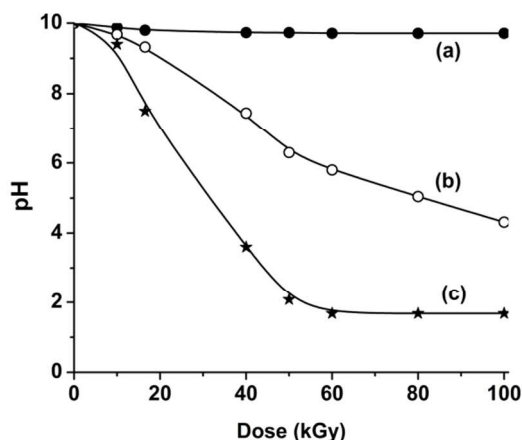


Fig. 5 Variation in the pH with different doses after gamma radiolysis of STDWW in the (a) absence and (b) presence of $K_2S_2O_8$ and (c) STDWW-SA in presence of $K_2S_2O_8$.

Conclusions

This study explores a reliable and promising way to use gamma radiolysis in presence of $K_2S_2O_8$ for complete mineralization of recalcitrant organics in to CO_2 and H_2O . Least amount of oxidant was required for gamma radiolysis in presence of $K_2S_2O_8$ to achieve the same extent of mineralization compared to photocatalysis, ozonolysis and general gamma radiolysis. The higher extent of mineralization of SDBS is not because of the conjugative effect of both $\cdot OH$ and $SO_4^{\cdot -}$ radicals, but because of the preferential formation of benzyl type of radicals via the formation of benzene radical cation. To the best of our knowledge, this study reports firstly the calculation of OCC for photocatalysis and gamma radiolysis for comparison with the efficiency of other AOPs. The use of H_2SO_4 in place of CH_3COOH in the pH adjustment step followed by the gamma radiolysis of STDWW in presence of $K_2S_2O_8$ is recommended for an effective effluent treatment process.

Notes and references

The authors wish to thank Dr. V. Kumar, RTDD, BARC for his kind interest in the work.

Notes and references

^a Radiation Technology Development Division, Bhabha Atomic Research Centre, Trombay, Mumbai-400 085, India. Fax: +91-22-2550-5151; Tel: +91-22-2559-0175; E-mail: paul.jhimli@gmail.com

^b Radiation and Photochemistry Division, Bhabha Atomic Research Centre, Trombay, Mumbai-400 085, India

1. I. Arslan, J. Hazard. Mater., 2001, **85**, 229-241.
2. I. Arslan-Alanton, I. Alaton, Ecotox. Environ. Safe., 2007, **68**, 98-107.
3. R.O. Cristovao, A.P.M. Tavares, J.M. Loureiro, R.A.R. Boaventura, E.A. Macedo, Bioresource Technol., 2009, **100**, 6236-6242.
4. J. Riu, I. Schonsee, D. Barcelo, Trends Anal. Chem., 1997, **16**, 405-419.
5. D. Georgiou, A. Aivazidis, J. Hatiras, K. Gimouhopoulas, Water Res., 2003, **37**, 2248-2250.

6. A. Pandey, P. Singh, L. Iyengar, Int. Biodeterior. Biodegrad., 2007, **59**, 73-84.
7. R. Andreozzi, V. Caprio, A. Insola, R. Marotta, Catal. Today, 1999, **53**, 51-59.
8. L. Wojnarovits, E. Takacs, Radiat. Phys. Chem., 2008, **77**, 225-244.
9. P.H. Chang, Water Sci. Technol., 2004, **49**, 213-218.
10. A. Anglada, A. Urtiaga, I. Ortiz, J. Chem. Technol. Biotechnol., 2009, **84**, 1747-1755.
11. T. Manson, J.P. Lorimer, Applied Sonochemistry: Uses in Chemistry and Processing, Wiley-VCH; 1st edition, 2002.
12. J.C. Crittenden, R.R. Trussell, D.W. Hand, G. Tchobanglouse, Water treatment principles and design. 2nd Ed, John Wiley and Sons, 2004.
13. J. Paul, D.B. Naik, S. Sabharwal, Radiat. Phys. Chem., 2010, **79**, 770-776.
14. J. Paul, K.P. Rawat, K.S.S. Sarma, S. Sabharwal, Appl. Radiat. Isotopes, 2011, **69**, 982-987.
15. M. Koch, A. Yediler, D. Lienert, G. Insel, A. Ketrupp, Chemosphere, 2002, **46**, 109-113.
16. G.V. Buxton, C.R. Stuart, J. Chem. Soc., Faraday Trans., 1995, **91**, 279-281.
17. U.G. Akapon, B.H. Hameed, J. Hazard. Mater., 2009, **170**, 520-529.
18. C. Jiang-Lin, L. Wen-Hua, Z. Jian-Qing, C. Chu-Nan, Acta Phys-Chim Sin., 2004, **20**, 735-739.
19. B. Kasprzyk-Hordern, M. Ziolk, J. Nawrocki, Appl. Catal. B: Environ., 2003, **46**, 639-669.
20. J. Hoigne, H. Bader, Water Res., 1976, **10**, 377-386.
21. N. Getoff, Radiat. Phys. Chem., 2002, **65**, 437-446.
22. J. Paul (Guin), D.B. Naik, Y.K. Bhardwaj, L. Varshney, Radiat. Phys. Chem., 2014, **100**, 38-44.
23. R.V. Bensasson, E.J. Land, T.G. Truscott, Pergamon Press, Oxford (1983) 1-19.
24. J. Paul, D.B. Naik, S. Sabharwal, Radiat. Phys. Chem., 2010, **79**, 770-776.
25. S. Liang, H.-W. Su, Ind. Eng. Chem. Res., 2009, **48**, 5558-5562.
26. J. Criquet, N.K.V. Leitner, Chem. Eng. J., 2011, **174**, 504-509.
27. P. Canizares, R. Paz, C. Saez, M.A. Radrigo, J. Environ. Manage., 2009, **90**, 410-420.
28. J. Mendez-Diaz, M. Sanchez-Polo, J. Rivera-Utrilla, S. Canonica, U.V. Gunten, Chem. Eng. J., 2010, **163**, 300-306.
29. E. Illes, E. Takacs, A. Dombi, K. Gajda-Schrantz, G. Racz, K. Gonter, L. Wojnarovits, Sci. Total Environ., 2013, **447**, 286-292.
30. S.M. Dockheer, L. Gubler, W.H. Koppenol, Phys. Chem. Chem. Phys., 2013, **15**, 4975-4983.
31. P. Neta, V. Madhavan, H. Zemel, R.W. Fessenden, J. Am. Chem. Soc., 1977, **99**, 163-164.
32. L. Osiewala, A. Socha, M. Wolszczak, J. Rynkowski, Radiat. Phys. Chem., 2013, **87**, 71-81.
33. H. Zemel, R.W. Fessenden, J. Phys. Chem., 1978, **82**, 2670-2676.
34. S. Venu, D.B. Naik, S.K. Sarkar, U.K. Aravind, A. Nijamudheen, C.T., Aravindakumar, J. Phys. Chem. A, 2013, **117**, 291-299.
35. J. Criquet, N.K.V. Leitner, Chemosphere, 2009, **77**, 194-200.
36. I. Greic, S. Papic, N. Koprivanak, I. Kovacic, Water Res., 2012, **46**, 5683-5695.